applied biosciences

MDPI

Review

Nature-Inspired Cellulose-Based Active Materials: From 2D to 4D

Marta I. Magalhães [1] and Ana P. C. Almeida [1,2,3,*]

[1] Laboratório Associado Para a Química Verde/Requimte, Department of Chemistry, NOVA School of Science and Technology, 2829-516 Caparica, Portugal
[2] CENIMAT | i3N, Department of Materials Science, School of Science and Technology, NOVA University Lisbon, 2829-516 Caparica, Portugal
[3] iBET—Instituto de Biologia Experimental e Tecnológica, Apartado 12, 2780-901 Oeiras, Portugal
* Correspondence: ana.almeida@fct.unl.pt

Abstract: Multifunctional materials and devices with captivating properties can be assembled from cellulose and cellulose-based composite materials combining functionality with structural performance. Cellulose is one of the most abundant renewable materials with captivating properties, such as mechanical robustness, biocompatibility, and biodegradability. Cellulose is a low-cost and abundant biodegradable resource, CO_2 neutral, with a wide variety of fibers available all over the world. Over thousands of years, nature has perfected cellulose-based materials according to their needs, such as function vs. structure. Mimicking molecular structures at the nano-, micro-, and macroscales existing in nature is a great strategy to produce synthetic cellulose-based active materials. A concise background of cellulose and its structural organization, as well as the nomenclature of cellulose nanomaterials, are first addressed. Key examples of nature-designed materials with unique characteristics, such as "eternal" coloration and water-induced movement are presented. The production of biomimetic fiber and 2D fiber-based cellulosic materials that have attracted significant attention within the scientific community are represented. Nature-inspired materials with a focus on functionality and response to an external stimulus are reported. Some examples of 3D-printed cellulosic materials bioinspired, reported recently in the literature, are addressed. Finally, printed cellulosic materials that morph from a 1D strand or 2D surface into a 3D shape, in response to an external stimulus, are reported. The purpose of this review is to discuss the most recent developments in the field of "nature-inspired" cellulose-based active materials regarding design, manufacturing, and inspirational sources that feature existing tendencies.

Keywords: cellulose; biomimetic; bioinspired; fibers; films; membranes; 4D printing

Citation: Magalhães, M.I.; Almeida, A.P.C. Nature-Inspired Cellulose-Based Active Materials: From 2D to 4D. *Appl. Biosci.* **2023**, *2*, 94–114. https://doi.org/10.3390/applbiosci2010009

Academic Editor: Robert Henry

Received: 20 January 2023
Revised: 8 March 2023
Accepted: 9 March 2023
Published: 15 March 2023

1. Introduction

Anselme Payen isolated cellulose, a water-insoluble substance, from green plants in 1838. Payen observed isomerism with starch and determined the empirical formula, $C_6H_{10}O_5$ by elemental analysis [1,2]. Some species of bacteria, such as the nonpathogenic bacteria *Komagataeibacter xylinus*, former Acetobacter, and Gluconacetobacter, can also produce cellulose [3–5]. In addition, cellulose can also be produced by some algae, oomycetes, the amoeboid protozoa *Dictyostelium discoideum*, and by a group of special marine animals, such as tunicates [6–8]. Clarification of the polymeric structure of cellulose can be traced back to 1920 with the revolutionary work of Hermann Staudinger [9]. Cellulose is composed of a *β-D*-glucopyranose unit linked by (1→4) glycosidic bonds, as can be observed in Figure 1. Cellulose is a main-chain polymer that results from the reaction of glucose molecules with the condensation of water. Cellulose is a linear-chain polymer that presents a large number of hydroxy groups (three per anhydroglucose unit (AGU)). In order to adjust the preferred bond angles of acetal oxygen bridges, every second AGU ring is rotated 180° in the plane. The repetitive unit of cellulose is cellobiose [10–12].

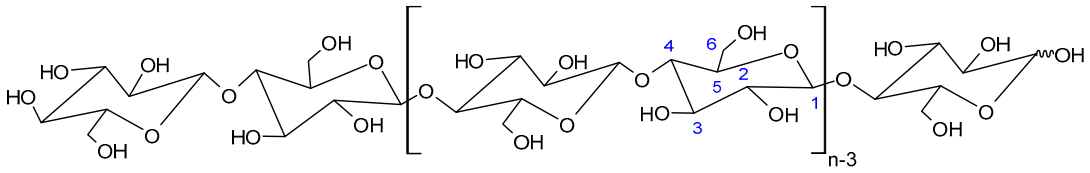

Figure 1. Molecular structure of cellulose (n = degree of polymerization). Cellobiose is the repetitive unit of cellulose, and the formation of hydrogen bonds is due to the existence of –OH.

The supramolecular structure of cellulose is responsible for its insolubility in water and in a large number of organic solvents. The supramolecular structure can be defined by the degree of crystallinity, crystallographic parameters, crystallite dimensions and presence of defects, structural indices of amorphous domains, and dimensions of fibrillar formations [13]. The physicochemical properties of cellulose are established by a particular hierarchical order in supramolecular structure and organization. The molecular structure conveys cellulose with its distinguishing properties, such as chirality, hydrophilicity, degradability, and extensive chemical variability, introduced by the high donor reactivity of the –OH groups [12]. One of the explanations for the stability of cellulose is that it exists generally in the form of crystals that have broad van der Waals attractive forces, as well as hydrogen bonds [14–16].

Interest in biobased materials, such as cellulosic materials, is continuously increasing in response to growing environmental awareness. Natural cellulose fibers that exhibit a wide range of sizes are excellent candidates to pave the way for the development of biobased high-performance materials with low environmental impact.

Cellulose Micro-/Nano- and Macroscale

Several studies have pursued isolation, characterization, and new applications for cellulose. Innovative approaches for their production scales from top-down methods, including enzymatic/chemical/physical methodologies using wood and forest/agricultural residues, to the bottom-up production of cellulose microfibrils by bacteria, have been presented. The cellulosic materials accomplished using these methodologies are commonly referred to as nanocelluloses [17]. The American Paper & Pulp Association (TAPPI WI 3021, Peachtree Corners, GA, USA) established a classification for nanocellulose based on the nanocellulose dimensions. The nomenclature, abbreviation, and dimensions defined for each group are described in Figure 2.

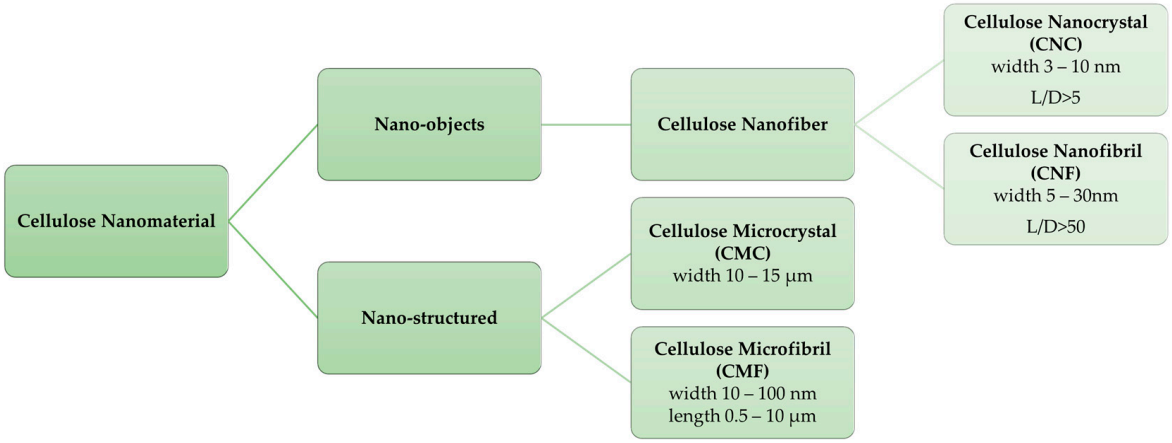

Figure 2. Standard terms established by The American Paper & Pulp Association (TAPPI WI 3021). Adapted from Ref. [18].

Cellulose microfibrils (CMF) can be obtained from suspensions of wood-based cellulose fibers using extensive mechanical methods, such as high-pressure homogenizers. This mechanical treatment delaminates the fibers and microfibrils with widths ranging from

10 to 100 μm and lengths ranging from 0.5 to 10 μm [18–20]. Cellulose nanofibrils (CNFs) are stretched aggregates of elementary nanofibrils that alternate with amorphous domains. The most common method to produce CNFs is through the mechanical delamination of softwood pulp in high-pressure homogenizers without any pretreatment or after chemical or enzymatic pretreatment. Pretreatments such as 2,2,6,6-tetramethylpiperidine-1-oxyl radical (TEMPO)-mediated oxidation, carboxymethylation, and mildly acidic or enzymatic cellulose hydrolysis, among others have been used to facilitate the mechanical disintegration process [21].

Cellulose nanocrystals (CNCs), also designated as nanowhiskers, consist of short, stiff, rod-like cellulose crystals [17,22–24]. According to The American Paper & Pulp Association (TAPPI WI 3021), the CNCs present widths in the range of 3–10 nm and aspect ratios larger than 5 and less than 50. They are obtained by the removal of amorphous sections of a purified cellulose source through acid hydrolysis [25], often followed by ultrasonic treatment. Disordered or amorphous regions of cellulose are favorably hydrolyzed, while crystalline regions that have higher resistance to acidic attack and cellulose rod-like nanocrystals are produced, as illustrated in the scheme presented in Figure 3.

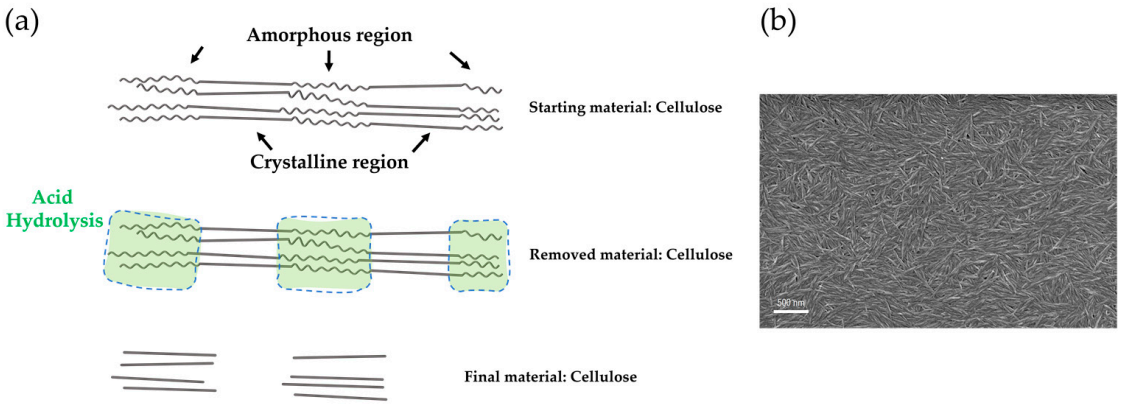

Figure 3. Cellulose nanomaterials: (**a**) schematic representation of the process to produce cellulose nanocrystals by means of acid hydrolysis, in which the amorphous regions are hydrolyzed and removed by the acid while the crystalline fractions are maintained. Adapted from Ref. [26]; (**b**) scanning electron microscopy image shows the top surface of a nanocrystalline cellulose freestanding film obtained by solvent casting of a CNC water suspension. Adapted with permission from Ref. [27]. Copyright 2020 Springer Nature B.V.

One of the oldest and most conventional procedures used to obtain CNCs consists of subjecting pure cellulosic material to strong acid hydrolysis under rigorously controlled conditions of temperature, agitation, and time [28]. For example, if the hydrolysis is performed with hydrogen chloride, HCl, weakly negatively charged particles are obtained, but if sulfuric acid, H_2SO_4, is used, the particles are more negatively charged, and approximately one-tenth of the glucose units can be functionalized with sulfate ester groups [17,24]. In both cases, the CNC suspension must be successively diluted with water and rinsed with consecutive centrifugations, to control the value of the pH of the suspension. Dialysis using distilled water is then accomplished to remove any free acid molecules from the dispersion. Additional steps such as filtration, differential centrifugation, or ultracentrifugation can also be used [17]. The dimensions of the crystals depend on the duration of the hydrolysis, and a longer reaction time produces shorter crystals [29]. The dimensions of the crystals produced are also dependent on the source and degree of crystallinity of the origin of cellulose [17]. The preparation of nanocellulose from cellulose requires two main stages. The first stage is dedicated to the pretreatment (chemical, physical, physicochemical, biolog-

ical, or combined) of feedstocks to obtain pure cellulose, whereas the second is dedicated to the transformation of cellulose to nanocellulose [28].

Bacterial nanocellulose (BNC) is produced by some species of bacteria, such as *Acetobacter*, *Acanthamoeba*, and *Achromobacter* spp. The molar mass, the molar mass distribution, and the supramolecular structure of the produced BNC can be controlled by selecting the substrates, cultivation conditions, various additives, and finally the bacterial strain. Quite a few strains of *K. xylinus* produce extracellular cellulose, a biofilm of varying thickness that is responsible for maintaining a high oxygenation of the colonies near the surface is formed, which also acts as a protective barrier against dehydration, natural enemies, and radiation [5]. In contrast to C and CNC isolated from cellulose sources, BNC is formed by the bacteria as a polymer and nanomaterial by biotechnological assembly processes, which involve a large number of genes coding individual enzymes and regulatory proteins [30], from low-molecular-weight carbon sources, such as *D*-glucose. BNC comprises a nonwoven nanofiber network, with fiber diameters spanning from 20 to 100 nm, and presents a remarkable water content of 99%. A high degree of polymerization and high crystallinity with values of 60–90% are also important features to mention in BNC [12,17].

In recent years, cellulose nanomaterials have been proven to be one of the most promising green materials in modern times. Their attractive characteristics, such as abundance, mechanical properties, renewability, biocompatibility, and high aspect ratio, have gained growing interest. Table 1 summarizes some examples of recent and emerging uses of cellulose nanomaterials in the field of biomedical engineering and materials science, which present high potential to be used in the near future by industry.

Table 1. Bioapplications using cellulose nanomaterials.

Cellulose Nanomaterial	Field of Application	Ref
Cellulose Nanocrystal (CNC)	Tissue regeneration	[31–33]
	Scaffolds	[34–38]
	Drug delivery systems	[39–43]
	Food industry	[44–48]
	Wound healing	[49–51]
Cellulose Nanofibril (CNF)	3D cell culture	[52–54]
	Drug delivery systems	[55–58]
	Food industry	[59,60]
	Tissue regeneration	[61–63]
Bacterial Nanocellulose (BNC)	Scaffolds	[64,65]
	Food packing	[66–68]
	Wound dressing	[69–71]
	Drug delivery systems	[72–75]

2. Nature-Designed Materials

Millions of years of natural selection have resulted in the design of cellulose-based structures that combine structure–function and are an inspiration for the production of synthetic materials. In this section, we describe some key examples of structures found in nature with unique characteristics, such as support, coloration, and movement. Plants present one interesting feature: the outer layer known as the cuticle, made of lipids embedded on a typically hydrophobic polymeric matrix [76], which can confer several properties to the plant. One of the most recognized examples is the self-cleaning mechanism present in the common lotus leaf. The micro- and nanostructured surface of the lotus leaf provides a highly effective antiadhesive effect, allowing the plant to protect itself against contamination [76]. Plants can also comprise, at different scales, anisotropic cellulose structures that are responsible for color and/or movement. These interesting features of plants inspired and continue to inspire scientists and engineers to pursue new biomimetic and actuating materials/devices that can change, for example, color and/or shape [77]. The majority of the colors that plants exhibit are due to pigments and dye molecules that are ephemeral and disappear with time [78,79]. Another approach used in the plant kingdom to

exhibit lively and attractive colors is accomplished by the interaction of light with ordered structures at the micron and nanoscale [80], defined as structural color. Iridescent colors, similar to the interference colors observed in soap bubbles or thin soap films [81,82], are colors that differ with the observing angle or lighting geometry; these features can also be observed in plants and result from ordered structures existing in the plants [83].

Whitney et al. [84] identified and explained that the iridescence observed in the *Hibiscus trionum* flower is attributed to a regular nanoscale pattern (striations or wrinkles) sculpted into the cuticle that covers the surface of the petal. These patterns present a biological purpose, since it was found that it could interact with its pollinators, predominantly bumblebees, through iridescent signals due to diffraction gratings [84]. Other authors determined that the microstructures embedded in the surface of the petals can act as a tactile signal used by the bees in the course of pollination to discriminate between different textures [85]. Structural colors do not disappear, and, in fruits, this permanent bright coloration increases the probability of dispersal [86]. A well-known example of structural coloration is the fruit from *Pollia condensata* preserved by Clark in the herbarium of the Royal Botanic Gardens, Kew, UK [86]. The fruit collected in 1974, continues to display its strong blue coloration. Vignolini et al. investigated its photonic response and reported that a multilayer helical structure composed of cellulose microfibrils is associated with the structural color presented by the fruit [86]. L *Margaritaria nobilis* fruit presents a structural iridescent green-blue color when fresh and a pearlescent color when dry. The color variation is reversible and is associated with the presence/absence of water in the fruit structure [87]. This performance is also assigned to a helical structure in the cell wall of the fruit. In the absence of water, the fruit dries, the seeds shrink, and a layer of air between the seeds and the endocarp is formed, blocking light absorption and decreasing the contrast. In the presence of water, the layer of air disappears due to fruit expansion, and the seeds interact with the endocarp, boosting the appearance of the blue-green color. Structural color has been more extensively studied in the animal kingdom, since there are several examples such as the cuticles of beetles, the wings of butterflies, and the feathers of numerous birds [88]. Animals shift their color for different reasons and by varied mechanisms. A well-known example is chameleons, which can suddenly modify their color to adjust to a new environment, to communicate, and to adjust temperature [89].

Micro- and nanofibers produced by plants are fundamental elements that assist in vital functions, for example, reproduction or weight support. Climbing plants are a notable example of organisms that use filaments as support; these structures are designated as tendrils. Darwin reported in 1865 that tendrils can create 2D structures (spirals) if they do not find a support point or 3D structures (helices) if they do [90]. Micro-nano-helical structures can also be found in water and the nutrient transport system and can be isolated from the leaves of different plants. For example, in *Agapanthus africanus* and *Ornithogalum thyrsoides*, the filaments are tightly coiled and present the same cellulosic skeleton but with different mechanical properties and surface morphology. These differences were revealed by the texture observed in nematic liquid crystal droplets pierced by these microfilaments [91]. Some advantages described for plants to exhibit helical structures are the enhancement of the mechanical properties and also the ability to present iridescent colors. In 2010, Murugesan et al. [92] developed a model based on the Landau–de Gennes theory, in which the helical arrangement of the plant cell wall presents improved mechanical resistance performance against the propagation of fractures by diverting the direction of the spread of cracks. The enhancement of the mechanical properties in structures composed of fibers that present helicoidal alignment was also reported by Tan et al. in 2017 [93].

Plant cell walls with crystalline cellulose microfibrils engrained in an amorphous matrix of polysaccharides, aromatic compounds, and structural proteins are the most common plant tissues that present hygroscopic behavior. A broad range of complex movements in plants can be triggered by numerous water-controlled actuators that combine different layers of cellulose [94,95]. The movements observed are due to anisotropic cellulose-based micro- and nanostructures that are specifically assembled to change shape

when the environmental conditions change [77]. Plant movements rely on differential water content within the plant cell tissues, i.e., the water is capable of flowing differently through the tissue, inflating the cells on one side and diminishing the cells on the other, therefore generating movement that can also exist in nonliving sections of plants, such as seeds and awns [96,97]. The steering forces for these mechanisms are the formation or breaking of hydrogen bonds and the entropic forces linked with the dilution of the molecular or macromolecular components. These swelling processes are easily mutable by controlling the humidity variations of the environment or changing the chemical potential of the swelling agent, since no intramolecular bonds are broken [97].

The seed-dispersal method of the true rose of Jericho, *Anastatica hierochuntica*, a desert plant, is correlated with the water-absorption-driven motion of the entire dead skeleton. The dead branches, which consist of dead cellulosic tissue, present a curling motion in the presence of water, allowing the fruit valves to open and release seeds. The closing process is associated with the rapid drying of the xylem vessels existent on the upper side of the stem [98,99]. The spike moss *Selaginella lepidophyla* also presents a water-driven motion, due to a different response to water by the inner and outer stems of the spike moss (Figure 4a). This type of movement is vital for plant survival, since it avoids photoinhibitory and thermal damage being a mechanism that overcomes stress due to sun radiation, high temperatures, and water scarcity. The water-driven movement of the stems can occur for several cycles without structural impairment. Water loss within the internal capillary spaces of parallel cellulose fibers in the cell walls, and the consequent shrinking of the cell wall is the driving force responsible for stem curling [100]. Pine cones can also fold their scales when moist air is present, and seed dispersion cannot occur, whereas in the absence of water, the scales open, and the seeds are released to be carried by the wind [101]. The asymmetrically oriented design of the cellulose fibrils in pine-cone scales is responsible for the conversion of local swelling/shrinking to a large-scale bending movement [102–104]. The presence of hygroscopic motion in coalified pine cones from the Eemian Interglacial period (≈126,000–113,000 years ago) and from the Middle Miocene period (≈16.5–11.5 million years ago) was reported by Poppinga et al. in 2017 [105].

Moist-driven movement is also abundant in plants that present spore dispersion. In the absence of water, the spores dry and deform, the sporangia (capsule in which the reproductive spores are produced and stored) opens, and the spores are released [106–108]. An interesting example is *Equisetum* spores, which present four flexible ribbon-like elaters (flexible ribbon-like limbs, designated elaters, that upon dehydration, unfold, and impel the spore). The elaters fold back in moist air; this mechanism allows the spores to move randomly [109]. Seedpods also present macroscopic deformations due to the nanoscale anisotropic expansion of their tissues. *Leucaena*, *Jacaranda*, and *Erythrina* pods open up over gradual bending and twisting in response to moisture absence (Figure 4b) [110]. The two initially flat pod valves curl into helical strips of opposite handedness. The pods present a layered structure composed of microfibrils oriented perpendicular to each other and at 45° to the pod axis. When the content of water in the tissues that constitute the pods decreases, the two layers shrink along perpendicular axes and shape distortion occurs [111,112]. A group of plants that also presents hygroscopic movement is the *Geraniaceae* family [113]. These plants are distinguished by the presence of a beak-like fruit. The moisture-driven helical movement of the *Erodium* (Figure 4c), a representative of this family, is due to the presence of the tilted helical configuration of the microfibrils in which the axis of the helix is at an angle to the long axis of the cell [113,114]. Consequently, changes in water content result in the coiling and uncoiling of the awn and self-burial of the seed [115–118].

Figure 4. Macroscopic moisture-driven deformation in plants: (**a**) Spike moss *Selaginella lepidophylla* hydrated state (**left**) and desiccate state (**right**). Adapted from Ref. [119]; (**b**) (**i**) *Leucaena*, (**ii**) *Jacaranda* and (**iii**) *Erythrina* seed pods; (**c**) *Erodium* seed and awn from the *Geraniaceae* family. Adapted from Ref. [113].

The term "nature inspired" is linked with the desire to understand, synthesize, and emulate a natural motif or phenomenon, to better understand nature. The scope of this review is to clarify and consolidate the knowledge and highlight emerging opportunities in cellulose-based active materials. The examples presented in the following sections, by no means exhaustive, were chosen among the innumerous works already reported, to exemplify the rich diversity of works on the production and development of fascinating multifunctional cellulose-based materials that merge functionality with structural performance using nature as inspiration.

3. Cellulose Biomimetic Fiber for Developing Functional Materials

Nature is full of extraordinary examples, some of them already mentioned previously in this review, of active materials with remarkable properties and performances. In this topic, the production of biomimetic fiber and fiber-based cellulosic materials that have attracted significant attention within the scientific community will be presented. The main strategy of biomimetic materials is to observe and understand the function of unique structures present in nature, and then use that knowledge to obtain similar structures and functionality. Jiang et al. [120] prepared cellulose membranes that can present a variety of predetermined deformations in the presence of moisture. Thin cellulose membranes from balsa wood fibers through a series of procedures that include chemical, mechanical, and heat treatment were prepared. The high humidity response presented by the thin membrane is due to a self-maintained moisture gradient induced by an asymmetric design of the membrane surfaces, strengthened by the hygroscopic swelling of the cellulose matrix. The authors designed and built a hydro-driven robot hand using these cellulose membranes. The hydro-driven robot hand could controllably grab and release objects 40 times heavier than its weight (Figure 5a). The high capability of load uptake is attributed to the fairly rigid cellulose elements in the membranes. These results are presented as a good option to achieve new smart structures and devices, such as flexible robots and self-unfolding structures produced from an environmentally friendly and recyclable source [120].

The scientific community has shown increased interest in the manufacture of electrospinning fibers. Using this process, it is possible to produce membranes and three-dimensional constructions with a wide range of polymers of different sizes and shapes and small pores. The fibers have diameters in the submicron range, and the surface area is remarkably high. Cao et al. [121] reported that it is possible to produce fiber-based nanoporous membranes that mimic spider webs using jute cellulose nanocrystals (CNCs) in their composition. For this purpose, different polyacrylonitrile (PAN), crosslinked polyvinyl alcohol (PVA), and silica membranes were produced using electrospinning. The electrospun membranes (Figure 5b) were later immersed in a solution of dodecyl trimethyl ammonium bromide (DTAB) and jute CNCs. The membranes obtained were produced using a low-energy consumption method and presented pores in the submicron range, very useful for ultrafiltration [121]. Later, also inspired by spider webs, Wang et al. [122] manufactured a fiber-based membrane composed of 48% functionalized sulfhydryl cellulose (SC) and polyacrylonitrile (PAN). The reusable membrane produced via electrospinning presented a great water–oil separation capability. To increase the concentration of cellulose nanocrystals that could be used, functionalized sulfhydryl cellulose nanocrystals were also added to the membrane composition. This strategy made it possible to manufacture ultrathin and porous membranes with better mechanical properties and with a separation efficiency of 99.9% [122].

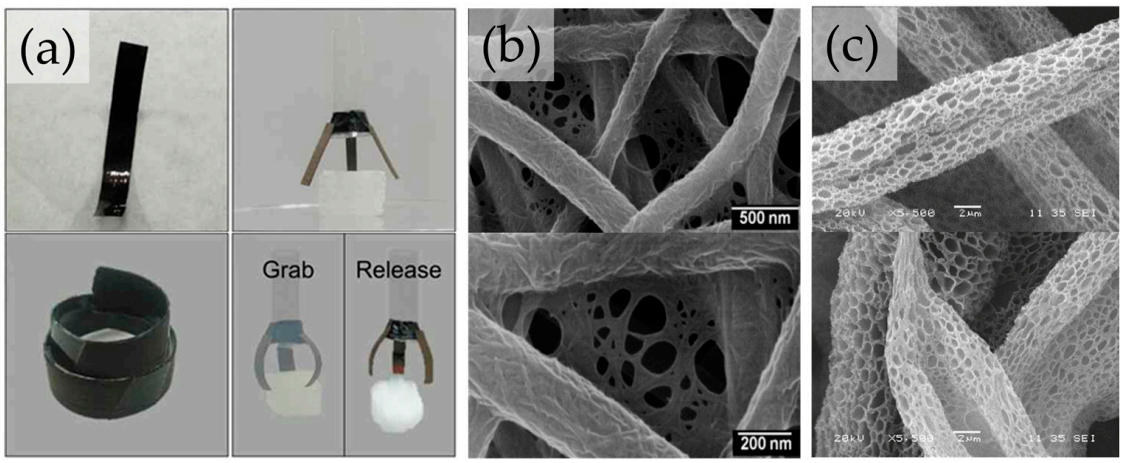

Figure 5. Biomimetic cellulosic fiber and fiber-based materials: (**a**) moisture-driven robot hand produced with balsa wood fibers. Adapted from Ref. [120]; (**b**) field-emission scanning electron micrograph of porous jute cellulose nanocrystals nanofibrous membranes. Adapted with permission from Ref. [121]. Copyright 2012 Elsevier; (**c**) scanning electron microscopy micrograph of porous cellulose acetate electrospun fibers. Adapted from Ref. [123].

Shigezawa et al. [124] were inspired by the water collection mechanism used by *Berkheya purpurea*. This plant, found in arid areas, has hydrophobic hairs (60–80 µm thick) and fine fibers (3–8 µm) to collect fresh water from the air. The authors mimicked this system using electrospinning to produce cellulose acetate fibers on a nylon mesh as support to capture water from fog. They studied different CA electrospinning times (10 s, 1 min, 5 min, 10 min) and concluded that the fibers electrospun for 1 min were the ones that had the best performance to capture water [124].

Electrospinning membranes have also begun to be used in tissue engineering with the aim of mimicking the extracellular matrix (ECM) to restore, maintain, or improve tissue function. Cellulose acetate membranes, produced using electrospinning, capable of mimicking this three-dimensional structure were reported by Han et al. [125]. These membranes will help in cell differentiation, tissue, and organ growth and also facilitate the cellular response [126]. Over the years, electrospun fibers of cellulose acetate combined with other polymers such as gelatin [127], polycaprolactone [128], polyvinyl alcohol [129], zein [130], and polyurethane [131] have been used in the field of wound-healing applica-

tions. An interesting example reported by Beikzadeh et al. [132] was the development of electrospinning membranes of cellulose acetate with encapsulated essential oil of lemon myrtle (LMEO), a natural antibacterial agent. It was proven that these membranes eradicated *Escherichia coli* and *Staphylococcus aureus* bacteria. In addition, the cellulose acetate membrane s released LMEO for a prolonged time, allowing the fibers to maintain their antimicrobial activity [132]. Laboy-López et al. [123] reported a bioactive cellulose acetate electrospun mat as a scaffold to replicate bone structure and promote tissue regeneration. A porous CA fiber mat (Figure 5c) was developed and chemically modified to bioactivate its surface in order to promote new tissue formation [123].

A smart moisture-wicking fabric produced with biomimetic micro- and nanofibrous Murray cellulosic membranes, with antigravity directional water transport and quick-dry performance for uninterrupted sweat release, was described by Wang et al. [133]. Moisture wicking is correlated with the capillarity force, which is responsible for driving the sweat through tiny capillary pores within the fabric. The authors used as inspiration the directional water transport systems present in nature, such as the hierarchical multibranching porous structure responsible for the transpiration in vascular plants, where the antigravity water movement from the soil to the plant stems and leaves happens by a passive wicking effect. The hierarchically porous membranes are produced using a bottom-up layer-by-layer deposition of three-layered fibrous membranes with multibranching macro-, micro-, and sub-micro-sized pores that comply with Murray's law. Murray's law states that the volumetric flow rate is proportional to the cube of the radius in a cylindrical channel optimized to require the minimum work to drive and maintain the fluid [134]. Murray membranes were prepared based on three criteria: antigravity directional water transport under differential capillary forces, ultrafast water transport and evaporation through hierarchical multibranching porous matrix, and extremely dry inner layer due to the surface energy gradient. Taking this into consideration the authors produced first an electrospun cellulose acetate fibrous membrane which is deposited on a polylactic acid nonwoven substrate. After that, the bilayer is dip-coated with microfibrilated cellulose, resulting in a three-layered leaf-vein-like nanofibrous membrane [133].

Guan et al. [135] reported a bacterial-cellulose-inspired lotus-fiber-like spiral-structure hydrogel, which they named biomimetic hydrogel fiber (BHF). BHF is described as a promising hydrogel fiber in biomedicine applications. Its exceptional stretchability and energy dissipation characteristics make it an ideal candidate for surgical sutures. BHF with lotus-fiber-mimetic spiral structure is built taking advantage of the bacterial cellulose hydrogel 3D cellulose nanofiber network [135].

4. Biomimetic Cellulosic Active Films

The development of nature-inspired materials with a focus on functionality and response to an external stimulus has been reported for several years. A one-step method to produce monolayer cellulose-based Janus-like membranes with reversible behavior of the micro-/nanostructures and solvent-responsive properties was reported by Liu and coworkers [136]. The structural difference among the top and bottom surfaces, due to the anisotropic self-assembly of cellulose nanocrystals (Figure 6a), enables the solvent-responsive curling of the film in different solvents with a rapidly reversible bending motion for many cycles [136]. Gevorkian et al. [137] reported a planar single-layer cellulose-based hydrogel with anisotropic structures. Shear-induced-orientation cellulose nanocrystals resulted in anisotropic mechanical and swelling properties of the cellulose hydrogel. Multiple complex 3D shapes from the same hydrogel were prepared according to the degree of its structural anisotropy [137]. Inspired by the plant movements triggered by the water content within nano- and mesoscale cellulose fibrillar structures, Wang and coworkers [138] developed a thin film of cellulose nanofibrils (CNFs) that presents humidity-controlled reversible actuation. To mimic the water-dependent curling and blooming of the glory flower, the authors prepared a four-petal CNF film "flower" that gradually folded the petals and that bloomed and recovered its original shape as a consequence of the presence or absence of

moisture, respectively. The curling and blooming mechanism is due to the formation of a dynamic bilayer-like structure in the thin film that comprises the difference between the water-swollen surface and the other surface [138].

Freestanding, flexible, and porous moisture-driven actuators inspired by *M. pudica* and pine cone were reported by Zhu et al. [139]. The active films consisted of poly (vinyl alcohol-*co*-ethylene) nanofibers and cellulose nanocrystals. The films prepared were applied to switches, soft robots, and humidity regulation. The locomotion of the actuator produced could be adjusted by cutting the film in different directions, and is a reflection of the orientation of the CNC existing in the film. The film could bend to an angle of 180° and recover its shape in less than 1 s for more than 100 cycles when the environment moisture decreased [139]. A flexible and flat photonic CNC with poly(ethylene glycol) (PEG) or glycerol composite films that present structural colors ranging from blue to red was reported by Duan et al. [140]. The CNC-PEG composite film presents reversible structural color change as the structure swells and dehydrates. The CNC-glycerol film presented diversified color changes in response to an external stimulus, depending on the content of the film additive. These films are described as low-cost materials suitable for colorimetric biosensors, optically active ingredients, inks, and decorative coatings [140].

Wu et al. developed a hyper-reflective, photonic cellulose nanocrystal-based nanocomposite film that mimics the shell structure of the *Chrysina* genus of beetles. The authors produced an asymmetric sandwich-like film by assembling hydrophilic cellulose nanocrystal (CNC) and poly(ethylene glycol) diacrylate (PEGDA) layers with a uniaxial orientation of the polyamide-6 layers. Humidity-triggered movement and variation of the reflected color is observed as a result of the asymmetric swelling of the hydrophilic components in the film, CNC and PEGDA. These interesting characteristics make this material suitable for color-changing sensors and actuators with a response in function of the environment [141].

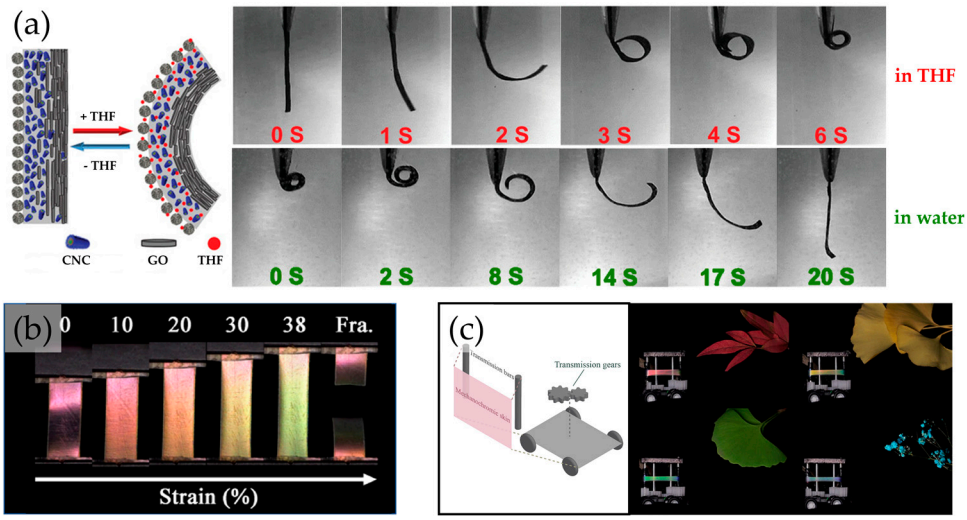

Figure 6. Cellulose-based active films: (**a**) cellulose-based Janus-like membranes composed of acylated cellulose nanocrystals (CNCs) and graphene oxide (GO) presenting solvent-responsive bending movement after exposed to tetrahydrofuran (THF) and water. Adapted from Ref. [136]; (**b**) optical photographs of the CNC/PEGDA film under deformation. Adapted with permission from Ref. [142]. Copyright 2020 American Chemical Society; (**c**) diagram of stealthy robot and photographs of the camouflage process of the CNC elastic film. Adapted with permission from Ref. [143]. Copyright 2020 American Chemical Society.

Motivated by the elastic skin of chameleons, Zhang et al. [142] developed a freestanding highly flexible film with structural color produced with cellulose nanocrystals in a poly(ethylene glycol)-based network. The biomimetic structural film showed reversible structural color change when stretched, visible to the naked eye (Figure 6b). The prepared films also presented water- and compression-responsive properties in controlled environ-

mental conditions. This bioinspired and biobased photonic film is described as suitable for chromogenic sensing, encryption, and anticounterfeit applications [142]. More recently, Zang et al. [143] also reported a ternary coassembly and post-UV-irradiation polymerization strategy to build a flexible and elastic CNC composite film that mimics chameleon skin. The smart skin produced presented the ability to adapt to the surrounding environment for camouflage simply by adjusting the stretching of the film (Figure 6c). The film presented vivid structural coloration and stretching-induced reversible color change from red to blue with relatively low stretching strain [143].

A biomimetic hydrogel based on CNCs inspired by human natural skin was produced by Lin et al. [144]. The simple method to develop a stretchable electronic device is by incorporating conductive polymers into a hydrogel matrix. The conductive polymers cannot tolerate large deformations; therefore, the authors added Ag nanoparticles into the hydrogel matrix composed of a polyvinyl alcohol (PVA) CNC system. To immobilize and stabilize the Ag nanoparticles on CNCs, the CNCs were initially coated with tannic acid (TA). The composite hydrogel presented enhanced conductive capability and stretchability, exceptional antibacterial properties, and repeatable self-healing capability. The hydrogels were manufactured into a flexible/self-healable capacitive sensor, and that was capable of sensing both large and subtle body motions, such as bending of joints, face expression, and breath, important features to replicate the tactual sensation of human skin [144].

Inspired by stomata, the structure existing in plant leaves responsible for the control of the rate of gas exchange, Hou et al. [145] prepared a bilayer intelligent hydrogel film. The authors presented a one-step casting strategy to produce an N-isopropylacrylamide/clay gel reinforced with a bacterial cellulose network. The anisotropic swelling promoted by the bilayer structure provided a rapid temperature-induced tunable shape modification with reversible behavior. As result, a bionic leaf stoma was built where the vapor could pass and fill the space above to achieve moisture circulation, as well as temperature and air balance. Moreover, taking into consideration the rapid shape transformation of the film, a circuit was built, and the film was used as a smart switch, where it was possible to accurately control the bending direction for turning the circuit on and off in a hygrothermal environment. This work presents a simple strategy to produce biomimetic actuators with applications in soft robotics, such as environmental regulation of temperature and moisture [145].

5. Printed 3D Structures

Traditional fabrication technologies struggle to accurately reproduce or imitate the complex structures existing in nature, which have specific mechanical, hydrodynamic, optical, and electrical properties. Three-dimensional (3D_ printing is reported as a suitable technology to fabricate structures with complex and arbitrary geometry [146,147]. The classification standards of the American Society for Testing and Materials (ASTM) define seven categories in 3D printing technology: powder bed fusion molding (PBF), material extrusion molding (ME), binder injection molding (BJ), photopolymerization curing, material inject forming (MJ), direct energy deposition (DED), and sheet lamination (SL) [148,149]. The standard term for 3D printing technologies and a description of each generalized term is represented in Table 2.

The most commonly used 3D bioprinting technologies are extrusion, injection, laser-assisted, fusion deposition, and direct ink writing [148]. In this topic, we will address some bioinspired examples of 3D-printed cellulosic materials recently reported in the literature.

In 2019, Kam et al. [150] reported a method called direct cryo writing (DCW) that combines freeze casting and 3D printing in a single step. The authors used an aqueous mixture of cellulose nanocrystals and xyloglucan to produce an aerogel with an internal structure mimicking plant cell walls. Directly printing onto a cold platform enables the direct post-processing of the resulting 3D-printed aerogel with aligned structures via lyophilization. DCW allows obtaining structures with a low solid content coupled with controlled porosity and tunable architecture, making this method suitable for the production of custom-designed biological scaffolds [150].

Table 2. Standard terms for 3D printing technologies. Please refer to the ISO/ASTM standard for a complete description of each generalized term [149], adapted with permission under a Creative Commons Attribution 4.0 International License [148].

Standard Term	Commercial Term	Description
PBF (Powder bed fusion molding)	SLS—Selective Laser Sintering SLM—Selective Laser Melting DMP—Direct Metal Printing DMLS—Direct Metal Laser Sintering EBM—Electron Beam Melting MJF—Multi Jet Fusion	Powder media is deposited on a build platform and subsequently bonded together through a heating process.
ME (Material extrusion molding)	FDM—Fused Deposition Modeling FFF—Fused Filament Fabrication	Material is dispensed, usually through a heated nozzle, onto a build platform.
BJ (Binder injection molding)	CJP—ProJet Color Jet Printing	Liquid agents are selectively dropped onto powder media. Subsequent infiltration or heating may be required.
Photopolymerization curing	SLA—Stereolithography apparatus DLP—Direct Light Processing CLIP—Continuous liquid interface production	Liquid photopolymer is selectively exposed to a light source facilitating layer-by-layer curing.
MJ (Material inject forming)	NPJ—Nanoparticle Jetting DOD—Drop-on-Demand PolyJet MJP—PolyJet Multijet Printing	A print head dispenses droplets of media, usually a photopolymer, onto a build platform where each layer is solidified or cured.
DED (Direct energy deposition)	LENS—Laser Engineered Net Shape EBAM—Electron Beam Additive Manufacture	Focused application of energy and material selectively melted and fused on a build platform or part.
SL (Sheet lamination)	LOM—Laminated Object Manufacturing	Discrete layers of material are fused or glued together to form a 3D object.

Three-dimensional (3D) bioprinting of a hierarchical nano- to macrofibrillary artificial human tissue with high resolution and integrity was reported by Mendes et al. [151]. The authors developed a nanocomposite bioink of platelet lysate hydrogel reinforced by cellulose nanocrystals, presented as suitable to print dynamic and personalized 3D living constructs that mimic the structure and composition of native tissues [151].

A lightweight (~90 mg/cm^3) and super-strong (16.6 MPa compressive Young's modulus) all-cellulose honeycomb structure, mimicking a paper wasp nest, was fabricated using direct-ink-writing 3D printing technology. The produced structure demonstrates superb elasticity and flexibility when wet, whereas the dried structure is a rigid and strong material capable of supporting 15,800 times its own weight. The authors describe this material as being applicable in biomedical, environmental, and structural engineering areas [152].

Two-layer cellulose-based scaffolds were 3D printed to mimic the osteochondral structure (bone structure), as reported by Guo et al. [153]. The scaffold consisted of a top pristine cellulose and a bottom cellulose/bioactive glass hydrogel. The printed scaffold exhibited superior performance for repairing the osteochondral defect by promoting osteoinduction and the formation of new bone inside the implanted scaffold. These results indicate that this cellulose-based printing system is suitable for application in tough tissue engineering applications [153].

Liu et al. reported a 3D-printed cellulose acetate nanoporous network that mimics water absorption in plant roots. The authors describe that this artificial root model produced using biomaterial-derived ink has immense potential for applications in plant science and bioengineering [154].

The possibility of 3D printing materials with nano/microscale orders was reported recently by Esmaeili et al. [155]. Three-dimensional (3D) complex geometries inspired by Bouligand structures, i.e., chiral arrangement of fibrous materials responsible for structural color in some beetles and berries, were produced using cellulose nanocrystal-based inks. The chiral assembly during the printing process is related to the shear forces inside the 3D printer's nozzle [155]. This biomimetic approach expands 3D printing beyond what has been reported so far.

6. 4D-Printed Cellulosic Responsive Materials

Four-dimensional (4D) printing is a one-step process, where time is considered the fourth dimension, in which the properties of the printed materials allow morphing a 1D strand or 2D surface into a 3D shape, or converting a 3D shape into another 3D shape, in response to an external stimulus such as the presence of water [156]. This technique was first introduced in 2013 by Skylar Tibbits at a TED conference [157]. As mentioned above, 4D printing can produce dynamic structures with adjustable shapes, properties, or functionality [158,159]. The 4D printing market is predicted to reach USD 510 million in the 2022–2030 period [160]. Gladman et al. [161] printed a series of functional folding-flower architectures using a biomimetic composite hydrogel with nanofibrillated cellulose. The printed material successfully reproduces the complex architecture of the orchid *Dendrobium helix*. The materials used present encoded anisotropy that promotes the appearance of an intricate shape when the printed structure is immersed in water [161]. Throughout the printing process, when the ink flows, fibril arrangement is induced, and anisotropic stiffness and longitudinal swelling are introduced in the structure. The printed programmable bilayer architecture enables petals to be closed or twisted upon swelling according to the orientation of the printed layers [161].

Siqueira et al. reported a monomer-based ink with cellulose CNCs dispersed in a mixture of 2-hydroxyethyl methacrylate (HEMA) monomer, polyether urethane acrylate, and a UV-light-cured photoinitiator, suitable for 3D printing. The structures printed with the inks showed shear-induced alignment of the CNC and enhanced stiffness along the printing direction. The authors state that this type of formulation is a suitable option for the biomimetic 4D printing of programmable reinforcer materials that can be reactive to external stimuli [162]. Natural fiber biocomposites are reported as a new class of smart materials, as they can be used in 4D printing to build unique shape-changing materials and structures. The fibers used in these biocomposites can be derived from hemp, flax, coconut, or wood [163–165].

Correia et al. described the printing of 4D pine scale and flap structures capable of multiphase movement [166]. This printed hydromorphic structure was structurally programmed and presented multiphase motion similar to that observed during the desiccation of natural pine cones (Figure 7a). The authors used 3D printing with a fused filament of wood polymer composite (fibrous filler from wood-derived fibers combined with co-polyester polymer matrix) and acrylonitrile butadiene styrene (ABS). The prepared composite mimics the properties of the swellable layer of the pine-cone scale, and the ABS acts as the stiffer and much less swellable layer, the resistance layer. The 4D-printed scales successfully exhibited a two-phase movement capable of recreating the natural scale behavior. The procedure used allowed defining local hygroscopic anisotropies and local nonhygroscopic movements that paved the way for the development of new advanced and passively actuating systems, with highly tailored shape-changing capabilities [166]. Mulakkal et al. developed a cellulose hydrogel composite ink to print a complex structure with predetermined layout rules to respond differently to hydration/dehydration. They used carboxymethylcellulose hydrocolloid with cellulose pulp fibers, also adding montmorillonite clay to the mixture to enhance the storage stability of the ink formulations and to facilitate the extrusion process during printing [167].

Wang et al. developed a starch, cellulose, and protein-based 2D film that changed to a 3D shape in the presence of moisture. The use of 4D printing in the food industry is of great interest since it can help to customize the product and develop unique characteristics that change in response to external stimuli such as flavors, textures, and aroma [168–170]. More recently, Lai et al. were capable of printing out a series of simple and complex morphing structures, using single ink, composed of a mixture of alginate and methylcellulose. By controlling the 2D architecture, the authors were able to obtain prescribed 3D morphologies after immersion in a calcium chloride solution (Figure 7b). The excellent printability combined with anisotropic swelling and consequent shape morphing of this cellulose-

based hydrogel makes it adequate to be used in tissue engineering, biomedical devices, and soft robotic fields [171].

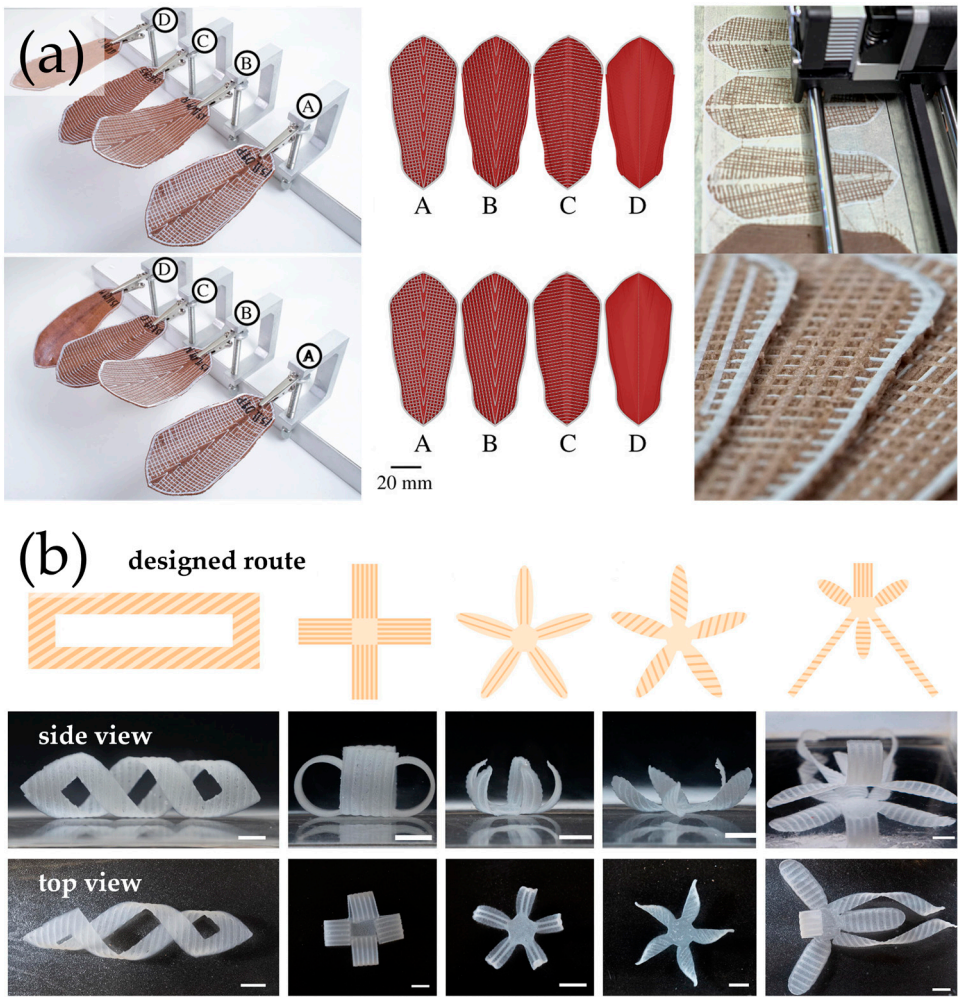

Figure 7. Four-dimensional (4D) printing inspired by nature structures of cellulosic materials: (**a**) 4D pine-scale-like structures capable of multiphase movement (**left**), according to several different predetermined patterns (**center**) using a 3D printer and a multimaterial process (**right**). Adapted with permission from Ref. [166]. Copyright 2020 The Royal Society; (**b**) designated 4D printed pattern alginate and methylcellulose hydrogel and their corresponding 3D complex structures from side and top view immersed in 0.1 M calcium chloride. Adapted from Ref. [171].

7. Conclusions and Future Directions

Stimuli-responsive nature-inspired cellulose-based materials have paved the way for a wide variety of applications, namely in actuators, sensors, soft robotics, biomedicine, tissue engineering, and smart fabrics. Cellulose and cellulose derivatives are easily available and low-cost polymers that have been widely used in commercial applications. Here, we have shown that cellulose and cellulose-based materials are excellent candidates to mimic the structures and functions existing in some plants and animals. The development of stable and innovative active materials/devices requires: (1) a full understanding of the underlying mechanisms after being exposed to external stimuli; (2) tunable fabrication of the smart cellulose-based materials; and (3) evaluation and continuous improvement of the active materials/devices performance regarding the desired sensitivity, specificity, and stability.

Cellulose has been used for centuries and will continue to be one of the most abundant natural polymeric sources for structural and functional materials. There is, therefore, no

doubt that the sprouting of the next generation of cellulose-based interactive materials inspired by nature will be in the markets within the next few years or decades.

Author Contributions: Conceptualization A.P.C.A.; writing—original draft preparation M.I.M. and A.P.C.A.; writing—review and editing A.P.C.A. All authors have read and agreed to the published version of the manuscript.

Funding: This work was supported by the Associate Laboratory for Green Chemistry—LAQV, which is financed by national funds from FCT/MCTES (UIDB/50006/2020 and UIDP/50006/2020) and financed by national funds from FCT—Fundação para a Ciência e a Tecnologia, I.P., in the scope of the projects LA/P/0037/2020, UIDP/50025/2020, and UIDB/50025/2020 of the Associate Laboratory Institute of Nanostructures, Nanomodelling and Nanofabrication—i3N. Ana Almeida is grateful for the financial support from Fundação para a Ciência e a Tecnologia (FCT), Portugal, through project 2022.01619.PTDC.

Institutional Review Board Statement: Not applicable.

Informed Consent Statement: Not applicable.

Data Availability Statement: Not applicable.

Conflicts of Interest: The authors declare no conflict of interest.

References

1. Payen, A. Mémoire sur la composition du tissu propre des plantes et du ligneux. *J. Comptes Rendus* **1838**, *7*, 1052–1056.
2. Fisher, C.H. Anselm Payen Pioneer in Natural Polymers and Industrial Chemistry. In *Pioneers in Polymer Science*; Seymour, R.B., Ed.; Springer: Dordrecht, The Netherlands, 1989; pp. 47–61. [CrossRef]
3. Brown, A.J. XIX.—The chemical action of pure cultivations of bacterium aceti. *J. Chem. Soc. Trans.* **1886**, *49*, 172–187. [CrossRef]
4. Ohad, I.; Danon, D.; Hestrin, S. Synthesis of Cellulose by Acetobacter Xylinum: V. Ultrastructure of Polymer. *J. Cell Biol.* **1962**, *12*, 31–46. [CrossRef] [PubMed]
5. Portela, R.; Leal, C.R.; Almeida, P.L.; Sobral, R.G. Bacterial cellulose: A versatile biopolymer for wound dressing applications. *Microb. Biotechnol.* **2019**, *12*, 586–610. [CrossRef] [PubMed]
6. Hol, H.R.; Jehli, J. The presence of cellulose microfibrils in the proteinaceous slime track of Dictyostelium discoideum. *Arch. Für Mikrobiol.* **1973**, *92*, 179–187. [CrossRef]
7. De Souza Lima, M.M.; Borsali, R. Static and Dynamic Light Scattering from Polyelectrolyte Microcrystal Cellulose†. *Langmuir* **2002**, *18*, 992–996. [CrossRef]
8. Dunlop, M.J.; Acharya, B.; Bissessur, R. Isolation of nanocrystalline cellulose from tunicates. *J. Environ. Chem. Eng.* **2018**, *6*, 4408–4412. [CrossRef]
9. Staudinger, H. Über Polymerisation. *Ber. Dtsch. Chem. Ges.* **1920**, *53*, 1073–1085. [CrossRef]
10. O'Sullivan, A.C. Cellulose: The structure slowly unravels. *Cellulose* **1997**, *4*, 173–207. [CrossRef]
11. Kamide, K. Characterization of Molecular Structure of Cellulose Derivatives. In *Cellulose and Cellulose Derivatives*; Kamide, K., Ed.; Elsevier: Amsterdam, The Netherlands, 2005; pp. 25–188. [CrossRef]
12. Klemm, D.; Heublein, B.; Fink, H.-P.; Bohn, A. Cellulose: Fascinating Biopolymer and Sustainable Raw Material. *Angew. Chem. Int. Ed.* **2005**, *44*, 3358–3393. [CrossRef]
13. Ioyelovich, M.Y. Supermolecular structure of native and isolated cellulose. *Polym. Sci. USSR* **1991**, *33*, 1670–1676. [CrossRef]
14. Bergenstråhle, M.; Wohlert, J.; Himmel, M.E.; Brady, J.W. Simulation studies of the insolubility of cellulose. *Carbohydr. Res.* **2010**, *345*, 2060–2066. [CrossRef]
15. French, A.D.; Concha, M.; Dowd, M.K.; Stevens, E.D. Electron (charge) density studies of cellulose models. *Cellulose* **2014**, *21*, 1051–1063. [CrossRef]
16. French, A.D.; Pérez, S.; Bulone, V.; Rosenau, T.; Gray, D. Cellulose. In *Encyclopedia of Polymer Science and Technology*; John Wiley & Sons: Hoboken, NJ, USA, 2018; pp. 1–69. [CrossRef]
17. Klemm, D.; Kramer, F.; Moritz, S.; Lindström, T.; Ankerfors, M.; Gray, D.; Dorris, A. Nanocelluloses: A New Family of Nature-Based Materials. *Angew. Chem. Int. Ed.* **2011**, *50*, 5438–5466. [CrossRef]
18. Mariano, M.; El Kissi, N.; Dufresne, A. Cellulose nanocrystals and related nanocomposites: Review of some properties and challenges. *J. Polym. Sci. Pol. Phys.* **2014**, *52*, 791–806. [CrossRef]
19. Turbak, A.F.; Snyder, F.W.; Sandberg, K.R. Microfibrillated cellulose, a new cellulose product: Properties, uses, and commercial potential. *J. Appl. Polym. Sci. Appl. Polym. Symp.* **1983**, *37*, 815–827.
20. Pääkkö, M.; Ankerfors, M.; Kosonen, H.; Nykänen, A.; Ahola, S.; Österberg, M.; Ruokolainen, J.; Laine, J.; Larsson, P.T.; Ikkala, O.; et al. Enzymatic Hydrolysis Combined with Mechanical Shearing and High-Pressure Homogenization for Nanoscale Cellulose Fibrils and Strong Gels. *Biomacromolecules* **2007**, *8*, 1934–1941. [CrossRef]

21. Ganapathy, V.; Muthukumaran, G.; Sudhagar, P.E.; Rashedi, A.; Norrrahim, M.N.F.; Ilyas, R.A.; Goh, K.L.; Jawaid, M.; Naveen, J. Mechanical properties of cellulose-based multiscale composites: A review. *Polym. Compos.* **2023**, *44*, 734–756. [CrossRef]
22. Ciolacu, D.E.; Darie, R.N. Nanocomposites Based on Cellulose, Hemicelluloses, and Lignin. In *Nanomaterials and Nanocomposites*; John Wiley & Sons: Hoboken, NJ, USA, 2016; pp. 391–424. [CrossRef]
23. Rojas, O.J. *Cellulose Chemistry and Properties: Fibers, Nanocelluloses and Advanced Materials*; Springer International Publishing: Berlin/Heidelberg, Germany, 2016.
24. Visakh, P.M. Introduction for Nanomaterials and Nanocomposites: State of Art, New Challenges, and Opportunities. In *Nanomaterials and Nanocomposites*; Wiley: Hoboken, NJ, USA, 2016; pp. 1–20. [CrossRef]
25. Bangar, S.P.; Harussani, M.M.; Ilyas, R.A.; Ashogbon, A.O.; Singh, A.; Trif, M.; Jafari, S.M. Surface modifications of cellulose nanocrystals: Processes, properties, and applications. *Food Hydrocoll.* **2022**, *130*, 107689. [CrossRef]
26. Mishra, R.K.; Sabu, A.; Tiwari, S.K. Materials chemistry and the futurist eco-friendly applications of nanocellulose: Status and prospect. *J. Saudi Chem. Soc.* **2018**, *22*, 949–978. [CrossRef]
27. Almeida, A.P.C.; Oliveira, J.; Fernandes, S.N.; Godinho, M.H.; Canejo, J.P. All-cellulose composite membranes for oil microdroplet collection. *Cellulose* **2020**, *27*, 4665–4677. [CrossRef]
28. Trache, D.; Tarchoun, A.F.; Derradji, M.; Hamidon, T.S.; Masruchin, N.; Brosse, N.; Hussin, M.H. Nanocellulose: From Fundamentals to Advanced Applications. *Front. Chem.* **2020**, *8*, 392. [CrossRef] [PubMed]
29. Beck-Candanedo, S.; Roman, M.; Gray, D.G. Effect of Reaction Conditions on the Properties and Behavior of Wood Cellulose Nanocrystal Suspensions. *Biomacromolecules* **2005**, *6*, 1048–1054. [CrossRef] [PubMed]
30. Barja, F. Bacterial nanocellulose production and biomedical applications. *J. Biomed. Res.* **2021**, *35*, 310–317. [CrossRef]
31. Maturavongsadit, P.; Paravyan, G.; Shrivastava, R.; Benhabbour, S.R. Thermo-/pH-responsive chitosan-cellulose nanocrystals based hydrogel with tunable mechanical properties for tissue regeneration applications. *Materialia* **2020**, *12*, 100681. [CrossRef]
32. Kamel, R.; El-Wakil, N.A.; Abdelkhalek, A.A.; Elkasabgy, N.A. Topical cellulose nanocrystals-stabilized nanoemulgel loaded with ciprofloxacin HCl with enhanced antibacterial activity and tissue regenerative properties. *J. Drug Deliv. Sci. Technol.* **2021**, *64*, 102553. [CrossRef]
33. Yang, W.; Zheng, Y.; Chen, J.; Zhu, Q.; Feng, L.; Lan, Y.; Zhu, P.; Tang, S.; Guo, R. Preparation and characterization of the collagen/cellulose nanocrystals/USPIO scaffolds loaded kartogenin for cartilage regeneration. *Mater. Sci. Eng. C* **2019**, *99*, 1362–1373. [CrossRef]
34. Patel, D.K.; Dutta, S.D.; Ganguly, K.; Lim, K.-T. Multifunctional bioactive chitosan/cellulose nanocrystal scaffolds eradicate bacterial growth and sustain drug delivery. *Int. J. Biol. Macromol.* **2021**, *170*, 178–188. [CrossRef]
35. Dutta, S.D.; Hexiu, J.; Patel, D.K.; Ganguly, K.; Lim, K.-T. 3D-printed bioactive and biodegradable hydrogel scaffolds of alginate/gelatin/cellulose nanocrystals for tissue engineering. *Int. J. Biol. Macromol.* **2021**, *167*, 644–658. [CrossRef]
36. Patel, D.K.; Dutta, S.D.; Hexiu, J.; Ganguly, K.; Lim, K.-T. Bioactive electrospun nanocomposite scaffolds of poly(lactic acid)/cellulose nanocrystals for bone tissue engineering. *Int. J. Biol. Macromol.* **2020**, *162*, 1429–1441. [CrossRef]
37. Shaheen, T.I.; Montaser, A.S.; Li, S. Effect of cellulose nanocrystals on scaffolds comprising chitosan, alginate and hydroxyapatite for bone tissue engineering. *Int. J. Biol. Macromol.* **2019**, *121*, 814–821. [CrossRef]
38. Luo, W.; Cheng, L.; Yuan, C.; Wu, Z.; Yuan, G.; Hou, M.; Chen, J.Y.; Luo, C.; Li, W. Preparation, characterization and evaluation of cellulose nanocrystal/poly(lactic acid) in situ nanocomposite scaffolds for tissue engineering. *Int. J. Biol. Macromol.* **2019**, *134*, 469–479. [CrossRef]
39. Yusefi, M.; Soon, M.L.-K.; Teow, S.-Y.; Monchouguy, E.I.; Neerooa, B.N.H.M.; Izadiyan, Z.; Jahangirian, H.; Rafiee-Moghaddam, R.; Webster, T.J.; Shameli, K. Fabrication of cellulose nanocrystals as potential anticancer drug delivery systems for colorectal cancer treatment. *Int. J. Biol. Macromol.* **2022**, *199*, 372–385. [CrossRef]
40. Long, W.; Ouyang, H.; Zhou, C.; Wan, W.; Yu, S.; Qian, K.; Liu, M.; Zhang, X.; Feng, Y.; Wei, Y. Simultaneous surface functionalization and drug loading: A novel method for fabrication of cellulose nanocrystals-based pH responsive drug delivery system. *Int. J. Biol. Macromol.* **2021**, *182*, 2066–2075. [CrossRef]
41. Kumari, P.; Seth, R.; Meena, A.; Sharma, D. Enzymatic synthesis of cellulose nanocrystals from lemongrass and its application in improving anti-cancer drug release, uptake and efficacy. *Ind. Crops Prod.* **2023**, *192*, 115933. [CrossRef]
42. Kumar, R.; Chauhan, S. Cellulose nanocrystals based delivery vehicles for anticancer agent curcumin. *Int. J. Biol. Macromol.* **2022**, *221*, 842–864. [CrossRef]
43. Gabriel, T.; Belete, A.; Hause, G.; Neubert, R.H.H.; Gebre-Mariam, T. Nanocellulose-based nanogels for sustained drug delivery: Preparation, characterization and in vitro evaluation. *J. Drug Deliv. Sci. Technol.* **2022**, *75*, 103665. [CrossRef]
44. Patiño Vidal, C.; Velásquez, E.; Galotto, M.J.; López de Dicastillo, C. Development of an antibacterial coaxial bionanocomposite based on electrospun core/shell fibers loaded with ethyl lauroyl arginate and cellulose nanocrystals for active food packaging. *Food Packag. Shelf Life* **2022**, *31*, 100802. [CrossRef]
45. Wu, Y.; Wu, W.; Farag, M.A.; Shao, P. Functionalized cellulose nanocrystal embedded into citrus pectin coating improves its barrier, antioxidant properties and potential application in food. *Food Chem.* **2023**, *401*, 134079. [CrossRef]
46. Halloub, A.; Raji, M.; Essabir, H.; Chakchak, H.; Boussen, R.; Bensalah, M.-o.; Bouhfid, R.; Qaiss, A.e.k. Intelligent food packaging film containing lignin and cellulose nanocrystals for shelf life extension of food. *Carbohydr. Polym.* **2022**, *296*, 119972. [CrossRef]
47. Lei, Y.; Yao, Q.; Jin, Z.; Wang, Y.-C. Intelligent films based on pectin, sodium alginate, cellulose nanocrystals, and anthocyanins for monitoring food freshness. *Food Chem.* **2023**, *404*, 134528. [CrossRef] [PubMed]

48. Mu, R.; Hong, X.; Ni, Y.; Li, Y.; Pang, J.; Wang, Q.; Xiao, J.; Zheng, Y. Recent trends and applications of cellulose nanocrystals in food industry. *Trends Food Sci. Technol.* **2019**, *93*, 136–144. [CrossRef]
49. Dong, D.; Chen, R.; Jia, J.; Zhao, C.; Chen, Z.; Lu, Q.; Sun, Y.; Huang, W.; Wang, C.; Li, Y.; et al. Tailoring and application of a multi-responsive cellulose nanofibre-based 3D nanonetwork wound dressing. *Carbohydr. Polym.* **2023**, *305*, 120542. [CrossRef] [PubMed]
50. Shi, X.; Chen, Z.; He, Y.; Lu, Q.; Chen, R.; Zhao, C.; Dong, D.; Sun, Y.; He, H. Dual light-responsive cellulose nanofibril-based in situ hydrogel for drug-resistant bacteria infected wound healing. *Carbohydr. Polym.* **2022**, *297*, 120042. [CrossRef] [PubMed]
51. Zhang, Q.; Zhu, J.; Jin, S.; Zheng, Y.; Gao, W.; Wu, D.; Yu, J.; Dai, Z. Cellulose-nanofibril-reinforced hydrogels with pH sensitivity and mechanical stability for wound healing. *Mater. Lett.* **2022**, *323*, 132596. [CrossRef]
52. Liu, J.; Cheng, F.; Grénman, H.; Spoljaric, S.; Seppälä, J.; Eriksson, J.E.; Willför, S.; Xu, C. Development of nanocellulose scaffolds with tunable structures to support 3D cell culture. *Carbohydr. Polym.* **2016**, *148*, 259–271. [CrossRef]
53. Li, Q.; Hatakeyama, M.; Kitaoka, T. Bioadaptive Porous 3D Scaffolds Comprising Cellulose and Chitosan Nanofibers Constructed by Pickering Emulsion Templating. *Adv. Funct. Mater.* **2022**, *32*, 2200249. [CrossRef]
54. Kim, H.J.; Oh, D.X.; Choy, S.; Nguyen, H.-L.; Cha, H.J.; Hwang, D.S. 3D cellulose nanofiber scaffold with homogeneous cell population and long-term proliferation. *Cellulose* **2018**, *25*, 7299–7314. [CrossRef]
55. Orasugh, J.T.; Saha, N.R.; Rana, D.; Sarkar, G.; Mollick, M.M.R.; Chattoapadhyay, A.; Mitra, B.C.; Mondal, D.; Ghosh, S.K.; Chattopadhyay, D. Jute cellulose nano-fibrils/hydroxypropylmethylcellulose nanocomposite: A novel material with potential for application in packaging and transdermal drug delivery system. *Ind. Crops Prod.* **2018**, *112*, 633–643. [CrossRef]
56. Zhao, J.; Lu, C.; He, X.; Zhang, X.; Zhang, W.; Zhang, X. Polyethylenimine-Grafted Cellulose Nanofibril Aerogels as Versatile Vehicles for Drug Delivery. *ACS Appl. Mater. Interfaces* **2015**, *7*, 2607–2615. [CrossRef]
57. Löbmann, K.; Svagan, A.J. Cellulose nanofibers as excipient for the delivery of poorly soluble drugs. *Int. J. Pharm.* **2017**, *533*, 285–297. [CrossRef]
58. Bhandari, J.; Mishra, H.; Mishra, P.K.; Wimmer, R.; Ahmad, F.J.; Talegaonkar, S. Cellulose nanofiber aerogel as a promising biomaterial for customized oral drug delivery. *Int. J. Nanomed.* **2017**, *12*, 2021–2031. [CrossRef]
59. Yu, Z.; Wang, W.; Kong, F.; Lin, M.; Mustapha, A. Cellulose nanofibril/silver nanoparticle composite as an active food packaging system and its toxicity to human colon cells. *Int. J. Biol. Macromol.* **2019**, *129*, 887–894. [CrossRef]
60. Yu, Z.; Dhital, R.; Wang, W.; Sun, L.; Zeng, W.; Mustapha, A.; Lin, M. Development of multifunctional nanocomposites containing cellulose nanofibrils and soy proteins as food packaging materials. *Food Packag. Shelf Life* **2019**, *21*, 100366. [CrossRef]
61. Kowalska-Ludwicka, K.; Cala, J.; Grobelski, B.; Sygut, D.; Jesionek-Kupnicka, D.; Kolodziejczyk, M.; Bielecki, S.; Pasieka, Z. Special paper—New method Modified bacterial cellulose tubes for regeneration of damaged peripheral nerves. *Arch. Med. Sci.* **2013**, *9*, 527–534. [CrossRef]
62. Pértile, R.; Moreira, S.; Andrade, F.; Domingues, L.; Gama, M. Bacterial cellulose modified using recombinant proteins to improve neuronal and mesenchymal cell adhesion. *Biotechnol. Prog.* **2012**, *28*, 526–532. [CrossRef]
63. Hwang, D.W.; Park, J.B.; Sung, D.; Park, S.; Min, K.-A.; Kim, K.W.; Choi, Y.; Kim, H.Y.; Lee, E.; Kim, H.S.; et al. 3D graphene-cellulose nanofiber hybrid scaffolds for cortical reconstruction in brain injuries. *2D Mater.* **2019**, *6*, 045043. [CrossRef]
64. Fey, C.; Betz, J.; Rosenbaum, C.; Kralisch, D.; Vielreicher, M.; Friedrich, O.; Metzger, M.; Zdzieblo, D. Bacterial nanocellulose as novel carrier for intestinal epithelial cells in drug delivery studies. *Mater. Sci. Eng. C* **2020**, *109*, 110613. [CrossRef]
65. Jaberifard, F.; Ghorbani, M.; Arsalani, N.; Mostafavi, H. A novel insoluble film based on crosslinked-starch with gelatin containing ZnO-loaded halloysite nanotube and bacterial nanocellulose for wound healing applications. *Appl. Clay Sci.* **2022**, *230*, 106667. [CrossRef]
66. Li, Q.; Gao, R.; Wang, L.; Xu, M.; Yuan, Y.; Ma, L.; Wan, Z.; Yang, X. Nanocomposites of Bacterial Cellulose Nanofibrils and Zein Nanoparticles for Food Packaging. *ACS Appl. Nano Mater.* **2020**, *3*, 2899–2910. [CrossRef]
67. Cazón, P.; Vázquez, M. Bacterial cellulose as a biodegradable food packaging material: A review. *Food Hydrocoll.* **2021**, *113*, 106530. [CrossRef]
68. Kamal, T.; Ul-Islam, M.; Fatima, A.; Ullah, M.W.; Manan, S. Cost-Effective Synthesis of Bacterial Cellulose and Its Applications in the Food and Environmental Sectors. *Gels* **2022**, *8*, 552. [CrossRef] [PubMed]
69. Almeida, A.P.C.; Saraiva, J.N.; Cavaco, G.; Portela, R.P.; Leal, C.R.; Sobral, R.G.; Almeida, P.L. Crosslinked bacterial cellulose hydrogels for biomedical applications. *Eur. Polym. J.* **2022**, *177*, 111438. [CrossRef]
70. Zhang, S.; Yang, Z.; Hao, J.; Ding, F.; Li, Z.; Ren, X. Hollow nanosphere-doped bacterial cellulose and polypropylene wound dressings: Biomimetic nanocatalyst mediated antibacterial therapy. *Chem. Eng. J.* **2022**, *432*, 134309. [CrossRef]
71. Resch, A.; Staud, C.; Radtke, C. Nanocellulose-based wound dressing for conservative wound management in children with second-degree burns. *Int. Wound J.* **2021**, *18*, 478–486. [CrossRef]
72. Jantarat, C.; Muenraya, P.; Srivaro, S.; Nawakitrangsan, A.; Promsornpason, K. Comparison of drug release behavior of bacterial cellulose loaded with ibuprofen and propranolol hydrochloride. *RSC Adv.* **2021**, *11*, 37354–37365. [CrossRef]
73. Beekmann, U.; Schmölz, L.; Lorkowski, S.; Werz, O.; Thamm, J.; Fischer, D.; Kralisch, D. Process control and scale-up of modified bacterial cellulose production for tailor-made anti-inflammatory drug delivery systems. *Carbohydr. Polym.* **2020**, *236*, 116062. [CrossRef]

74. Meneguin, A.B.; da Silva Barud, H.; Sábio, R.M.; de Sousa, P.Z.; Manieri, K.F.; de Freitas, L.A.P.; Pacheco, G.; Alonso, J.D.; Chorilli, M. Spray-dried bacterial cellulose nanofibers: A new generation of pharmaceutical excipient intended for intestinal drug delivery. *Carbohydr. Polym.* **2020**, *249*, 116838. [CrossRef]
75. Park, D.; Kim, J.W.; Shin, K.; Kim, J.W. Bacterial cellulose nanofibrils-reinforced composite hydrogels for mechanical compression-responsive on-demand drug release. *Carbohydr. Polym.* **2021**, *272*, 118459. [CrossRef]
76. Barthlott, W.; Neinhuis, C. Purity of the sacred lotus, or escape from contamination in biological surfaces. *Planta* **1997**, *202*, 1–8. [CrossRef]
77. Oliver, K.; Seddon, A.; Trask, R.S. Morphing in nature and beyond: A review of natural and synthetic shape-changing materials and mechanisms. *J. Mater. Sci.* **2016**, *51*, 10663–10689. [CrossRef]
78. Ball, P. Botanists' blues. *Nature* **2007**, *449*, 982. [CrossRef]
79. Lee, D. *Nature's Palette: The Science of Plant Color*; University of Chicago Press: Chicago, IL, USA, 2010.
80. Vukusic, P.; Sambles, J.R. Photonic structures in biology. *Nature* **2003**, *424*, 852–855. [CrossRef]
81. Doucet, S.M.; Meadows, M.G. Iridescence: A functional perspective. *J. R. Soc. Interface* **2009**, *6* (Suppl. S2), S115–S132. [CrossRef]
82. Gruson, H.; Andraud, C.; Marcillac, W.D.d.; Berthier, S.; Elias, M.; Gomez, D. Quantitative characterization of iridescent colours in biological studies: A novel method using optical theory. *Interface Focus* **2019**, *9*, 20180049. [CrossRef]
83. Morris, R.B. Iridescence from diffraction structures in the wing scales of Callophrys rubi, the Green Hairstreak. *J. Entomol. Ser. A Gen. Entomol.* **1975**, *49*, 149–154. [CrossRef]
84. Whitney, H.M.; Kolle, M.; Andrew, P.; Chittka, L.; Steiner, U.; Glover, B.J. Floral iridescence, produced by diffractive optics, acts as a cue for animal pollinators. *Science* **2009**, *323*, 130–133. [CrossRef]
85. Kevan, P.G.; Lane, M.A. Flower petal microtexture is a tactile cue for bees. *Proc. Natl. Acad. Sci. USA* **1985**, *82*, 4750–4752. [CrossRef]
86. Vignolini, S.; Rudall, P.J.; Rowland, A.V.; Reed, A.; Moyroud, E.; Faden, R.B.; Baumberg, J.J.; Glover, B.J.; Steiner, U. Pointillist structural color in Pollia fruit. *Proc. Natl. Acad. Sci. USA* **2012**, *109*, 15712–15715. [CrossRef]
87. Vignolini, S.; Gregory, T.; Kolle, M.; Lethbridge, A.; Moyroud, E.; Steiner, U.; Glover, B.J.; Vukusic, P.; Rudall, P.J. Structural colour from helicoidal cell-wall architecture in fruits of *Margaritaria nobilis*. *J. R. Soc. Interface* **2016**, *13*, 20160645. [CrossRef]
88. Almeida, A.P.C.; Canejo, J.P.; Fernandes, S.N.; Echeverria, C.; Almeida, P.L.; Godinho, M.H. Cellulose-Based Biomimetics and Their Applications. *Adv. Mater.* **2018**, *30*, 1703655. [CrossRef]
89. Ligon, R.A.; McGraw, K.J. Chameleons communicate with complex colour changes during contests: Different body regions convey different information. *Biol. Lett.* **2013**, *9*, 20130892. [CrossRef] [PubMed]
90. Darwin, C. *The Movements and Habits of Climbing Plants*; John Murray: London, UK, 1875.
91. Almeida, A.P.; Canejo, J.; Mur, U.; Čopar, S.; Almeida, P.L.; Žumer, S.; Godinho, M.H. Spotting plants' microfilament morphologies and nanostructures. *Proc. Natl. Acad. Sci. USA* **2019**, *116*, 13188–13193. [CrossRef] [PubMed]
92. Murugesan, Y.K.; Rey, A.D. Modeling Textural Processes during Self-Assembly of Plant-Based Chiral-Nematic Liquid Crystals. *Polymers* **2010**, *2*, 766–785. [CrossRef]
93. Tan, T.; Ribbans, B. A bioinspired study on the compressive resistance of helicoidal fibre structures. *Proc. R. Soc. A Math. Phys. Eng. Sci.* **2017**, *473*, 20170538. [CrossRef]
94. Fratzl, P.; Elbaum, R.; Burgert, I. Cellulose fibrils direct plant organ movements. *Faraday Discuss.* **2008**, *139*, 275–282. [CrossRef]
95. Elbaum, R.; Abraham, Y. Insights into the microstructures of hygroscopic movement in plant seed dispersal. *Plant Sci.* **2014**, *223*, 124–133. [CrossRef]
96. Lacey, E.P.; Kaufman, P.B.; Dayanandan, P. The Anatomical Basis for Hygroscopic Movement in Primary Rays of Daucus carota Ssp. carota (Apiaceae). *Bot. Gaz.* **1983**, *144*, 371–375. [CrossRef]
97. Bertinetti, L.; Fischer, F.D.; Fratzl, P. Physicochemical Basis for Water-Actuated Movement and Stress Generation in Nonliving Plant Tissues. *Phys. Rev. Lett.* **2013**, *111*, 238001. [CrossRef]
98. Friedman, J.; Gunderman, N.; Ellis, M. Water response of the hygrochastic skeletons of the true rose of Jericho (*Anastatica hierochuntica* L.). *Oecologia* **1978**, *32*, 289–301. [CrossRef]
99. Hegazy, A.K.; Barakat, H.N.; Kabiel, H.F. Anatomical significance of the hygrochastic movement in Anastatica hierochuntica. *Ann. Bot.* **2006**, *97*, 47–55. [CrossRef]
100. Lebkuecher, J.G.; Eickmeier, W.G. Reduced photoinhibition with stem curling in the resurrection plant Selaginella lepidophylla. *Oecologia* **1991**, *88*, 597–604. [CrossRef]
101. Le Duigou, A.; Castro, M. Evaluation of force generation mechanisms in natural, passive hydraulic actuators. *Sci. Rep.* **2016**, *6*, 18105. [CrossRef]
102. Dawson, C.; Vincent, J.F.V.; Rocca, A.-M. How pine cones open. *Nature* **1997**, *390*, 668. [CrossRef]
103. Song, K.; Yeom, E.; Seo, S.-J.; Kim, K.; Kim, H.; Lim, J.-H.; Joon Lee, S. Journey of water in pine cones. *Sci. Rep.* **2015**, *5*, 9963. [CrossRef]
104. Song, K.; Chang, S.-S.; Lee, S.J. How the pine seeds attach to/detach from the pine cone scale? *Front. Life Sci.* **2017**, *10*, 38–47. [CrossRef]
105. Poppinga, S.; Nestle, N.; Šandor, A.; Reible, B.; Masselter, T.; Bruchmann, B.; Speck, T. Hygroscopic motions of fossil conifer cones. *Sci. Rep.* **2017**, *7*, 40302. [CrossRef]
106. Newcombe, F.C.J.B.G. Spore-dissemination of Equisetum. *Bot. Gaz.* **1888**, *13*, 173–178. [CrossRef]

107. Katifori, E.; Alben, S.; Cerda, E.; Nelson, D.R.; Dumais, J. Foldable structures and the natural design of pollen grains. *Proc. Natl. Acad. Sci. USA* **2010**, *107*, 7635–7639. [CrossRef]
108. Noblin, X.; Rojas, N.O.; Westbrook, J.; Llorens, C.; Argentina, M.; Dumais, J. The Fern Sporangium: A Unique Catapult. *Science* **2012**, *335*, 1322. [CrossRef]
109. Marmottant, P.; Ponomarenko, A.; Bienaimé, D. The walk and jump of Equisetum spores. *Proc. R. Soc. B Biol. Sci.* **2013**, *280*, 20131465. [CrossRef] [PubMed]
110. Bar-On, B.; Sui, X.; Livanov, K.; Achrai, B.; Kalfon-Cohen, E.; Wiesel, E.; Wagner, H.D. Structural origins of morphing in plant tissues. *Appl. Phys. Lett.* **2014**, *105*, 033703. [CrossRef]
111. Ghafouri, R.; Bruinsma, R. Helicoid to Spiral Ribbon Transition. *Phys. Rev. Lett.* **2005**, *94*, 138101. [CrossRef] [PubMed]
112. Armon, S.; Efrati, E.; Kupferman, R.; Sharon, E. Geometry and mechanics in the opening of chiral seed pods. *Science* **2011**, *333*, 1726–1730. [CrossRef] [PubMed]
113. Abraham, Y.; Elbaum, R. Hygroscopic movements in Geraniaceae: The structural variations that are responsible for coiling or bending. *New Phytol.* **2013**, *199*, 584–594. [CrossRef]
114. Almeida, A.P.C.; Querciagrossa, L.; Silva, P.E.S.; Gonçalves, F.; Canejo, J.P.; Almeida, P.L.; Godinho, M.H.; Zannoni, C. Reversible water driven chirality inversion in cellulose-based helices isolated from Erodium awns. *Soft Matter* **2019**, *15*, 2838–2847. [CrossRef]
115. Jung, W.; Kim, W.; Kim, H.Y. Self-burial mechanics of hygroscopically responsive awns. *Integr. Comp. Biol.* **2014**, *54*, 1034–1042. [CrossRef]
116. Zhao, C.; Liu, Q.; Ren, L.; Song, Z.; Wang, J. A 3D micromechanical study of hygroscopic coiling deformation in Pelargonium seed: From material and mechanics perspective. *J. Mater. Sci.* **2017**, *52*, 415–430. [CrossRef]
117. Stamp, N.E. Self-Burial Behaviour of Erodium Cicutarium Seeds. *J. Ecol.* **1984**, *72*, 611–620. [CrossRef]
118. Elbaum, R.; Gorb, S.; Fratzl, P. Structures in the cell wall that enable hygroscopic movement of wheat awns. *J. Struct. Biol.* **2008**, *164*, 101–107. [CrossRef]
119. Rafsanjani, A.; Brulé, V.; Western, T.L.; Pasini, D. Hydro-Responsive Curling of the Resurrection Plant Selaginella lepidophylla. *Sci. Rep.* **2015**, *5*, 8064. [CrossRef]
120. Jiang, X.; Tian, B.; Xuan, X.; Zhou, W.; Zhou, J.; Chen, Y.; Lu, Y.; Zhang, Z. Cellulose membranes as moisture-driven actuators with predetermined deformations and high load uptake. *Int. J. Smart Nano Mater.* **2021**, *12*, 146–156. [CrossRef]
121. Cao, X.; Wang, X.; Ding, B.; Yu, J.; Sun, G. Novel spider-web-like nanoporous networks based on jute cellulose nanowhiskers. *Carbohydr. Polym.* **2013**, *92*, 2041–2047. [CrossRef]
122. Wang, Q.; Wang, D.; Cheng, W.; Huang, J.; Cao, M.; Niu, Z.; Zhao, Y.; Yue, Y.; Han, G. Spider-web-inspired membrane reinforced with sulfhydryl-functionalized cellulose nanocrystals for oil/water separation. *Carbohydr. Polym.* **2022**, *282*, 119049. [CrossRef]
123. Laboy-López, S.; Méndez Fernández, P.O.; Padilla-Zayas, J.G.; Nicolau, E. Bioactive Cellulose Acetate Electrospun Mats as Scaffolds for Bone Tissue Regeneration. *Int. J. Biomater.* **2022**, *2022*, 3255039. [CrossRef]
124. Shigezawa, N.; Ito, F.; Murakami, Y.; Yamanaka, S.; Morikawa, H. Development of combination textile of thin and thick fiber for fog collection bioinspired by Burkheya purpurea. *J. Text. Inst.* **2016**, *107*, 1014–1021. [CrossRef]
125. Han, D.; Gouma, P.-I. Electrospun bioscaffolds that mimic the topology of extracellular matrix. *Nanomed. Nanotechnol. Biol. Med.* **2006**, *2*, 37–41. [CrossRef]
126. Gruppuso, M.; Turco, G.; Marsich, E.; Porrelli, D. Polymeric wound dressings, an insight into polysaccharide-based electrospun membranes. *Appl. Mater. Today* **2021**, *24*, 101148. [CrossRef]
127. Vatankhah, E.; Prabhakaran, M.P.; Jin, G.; Mobarakeh, L.G.; Ramakrishna, S. Development of nanofibrous cellulose acetate/gelatin skin substitutes for variety wound treatment applications. *J. Biomater. Appl.* **2014**, *28*, 909–921. [CrossRef]
128. Liao, N.; Unnithan, A.R.; Joshi, M.K.; Tiwari, A.P.; Hong, S.T.; Park, C.-H.; Kim, C.S. Electrospun bioactive poly (ε-caprolactone)–cellulose acetate–dextran antibacterial composite mats for wound dressing applications. *Colloids Surf. A Physicochem. Eng. Asp.* **2015**, *469*, 194–201. [CrossRef]
129. Gaydhane, M.K.; Kanuganti, J.S.; Sharma, C.S. Honey and curcumin loaded multilayered polyvinylalcohol/cellulose acetate electrospun nanofibrous mat for wound healing. *J. Mater. Res.* **2020**, *35*, 600–609. [CrossRef]
130. Liu, F.; Li, X.; Wang, L.; Yan, X.; Ma, D.; Liu, Z.; Liu, X. Sesamol incorporated cellulose acetate-zein composite nanofiber membrane: An efficient strategy to accelerate diabetic wound healing. *Int. J. Biol. Macromol.* **2020**, *149*, 627–638. [CrossRef] [PubMed]
131. Esmaeili, E.; Eslami-Arshaghi, T.; Hosseinzadeh, S.; Elahirad, E.; Jamalpoor, Z.; Hatamie, S.; Soleimani, M. The biomedical potential of cellulose acetate/polyurethane nanofibrous mats containing reduced graphene oxide/silver nanocomposites and curcumin: Antimicrobial performance and cutaneous wound healing. *Int. J. Biol. Macromol.* **2020**, *152*, 418–427. [CrossRef] [PubMed]
132. Beikzadeh, S.; Akbarinejad, A.; Swift, S.; Perera, J.; Kilmartin, P.A.; Travas-Sejdic, J. Cellulose acetate electrospun nanofibers encapsulating Lemon Myrtle essential oil as active agent with potent and sustainable antimicrobial activity. *React. Funct. Polym.* **2020**, *157*, 104769. [CrossRef]
133. Wang, X.; Huang, Z.; Miao, D.; Zhao, J.; Yu, J.; Ding, B. Biomimetic Fibrous Murray Membranes with Ultrafast Water Transport and Evaporation for Smart Moisture-Wicking Fabrics. *ACS Nano* **2019**, *13*, 1060–1070. [CrossRef]
134. Murray, C.D. The Physiological Principle of Minimum Work: I. The Vascular System and the Cost of Blood Volume. *Proc. Natl. Acad. Sci. USA* **1926**, *12*, 207–214. [CrossRef]

135. Guan, Q.-F.; Han, Z.-M.; Zhu, Y.; Xu, W.-L.; Yang, H.-B.; Ling, Z.-C.; Yan, B.-B.; Yang, K.-P.; Yin, C.-H.; Wu, H.; et al. Bio-Inspired Lotus-Fiber-like Spiral Hydrogel Bacterial Cellulose Fibers. *Nano Lett.* **2021**, *21*, 952–958. [CrossRef]
136. Liu, H.; Pang, B.; Tang, Q.; Müller, M.; Zhang, H.; Dervişoğlu, R.; Zhang, K. Self-Assembly of Surface-Acylated Cellulose Nanowhiskers and Graphene Oxide for Multiresponsive Janus-Like Films with Time-Dependent Dry-State Structures. *Small* **2020**, *16*, 2004922. [CrossRef]
137. Gevorkian, A.; Morozova, S.M.; Kheiri, S.; Khuu, N.; Chen, H.; Young, E.; Yan, N.; Kumacheva, E. Actuation of Three-Dimensional-Printed Nanocolloidal Hydrogel with Structural Anisotropy. *Adv. Funct. Mater.* **2021**, *31*, 2010743. [CrossRef]
138. Wang, M.; Tian, X.; Ras, R.H.A.; Ikkala, O. Sensitive Humidity-Driven Reversible and Bidirectional Bending of Nanocellulose Thin Films as Bio-Inspired Actuation. *Adv. Mater. Interfaces* **2015**, *2*, 1500080. [CrossRef]
139. Zhu, Q.; Jin, Y.; Wang, W.; Sun, G.; Wang, D. Bioinspired Smart Moisture Actuators Based on Nanoscale Cellulose Materials and Porous, Hydrophilic EVOH Nanofibrous Membranes. *ACS Appl. Mater. Interfaces* **2019**, *11*, 1440–1448. [CrossRef]
140. Duan, R.; Lu, M.; Tang, R.; Guo, Y.; Zhao, D. Structural Color Controllable Humidity Response Chiral Nematic Cellulose Nanocrystalline Film. *Biosensors* **2022**, *12*, 707. [CrossRef]
141. Wu, T.; Li, J.; Li, J.; Ye, S.; Wei, J.; Guo, J. A bio-inspired cellulose nanocrystal-based nanocomposite photonic film with hyper-reflection and humidity-responsive actuator properties. *J. Mater. Chem. C* **2016**, *4*, 9687–9696. [CrossRef]
142. Zhang, Z.-L.; Dong, X.; Fan, Y.-N.; Yang, L.-M.; He, L.; Song, F.; Wang, X.-L.; Wang, Y.-Z. Chameleon-Inspired Variable Coloration Enabled by a Highly Flexible Photonic Cellulose Film. *ACS Appl. Mater. Interfaces* **2020**, *12*, 46710–46718. [CrossRef]
143. Zhang, Z.-L.; Dong, X.; Zhao, Y.-Y.; Song, F.; Wang, X.-L.; Wang, Y.-Z. Bioinspired Optical Flexible Cellulose Nanocrystal Films with Strain-Adaptive Structural Coloration. *Biomacromolecules* **2022**, *23*, 4110–4117. [CrossRef]
144. Lin, F.; Wang, Z.; Shen, Y.; Tang, L.; Zhang, P.; Wang, Y.; Chen, Y.; Huang, B.; Lu, B. Natural skin-inspired versatile cellulose biomimetic hydrogels. *J. Mater. Chem. A* **2019**, *7*, 26442–26455. [CrossRef]
145. Hou, K.; Nie, Y.; Tendo Mugaanire, I.; Guo, Y.; Zhu, M. A novel leaf inspired hydrogel film based on fiber reinforcement as rapid steam sensor. *Chem. Eng. J.* **2020**, *382*, 122948. [CrossRef]
146. Spadaccini, C.M. Additive manufacturing and processing of architected materials. *Mater. Res. Soc. Bull.* **2019**, *44*, 782–788. [CrossRef]
147. Wang, D.; Chen, D.; Chen, Z. Recent Progress in 3D Printing of Bioinspired Structures. *Front. Mater.* **2020**, *7*, 286. [CrossRef]
148. Alexander, A.E.; Wake, N.; Chepelev, L.; Brantner, P.; Ryan, J.; Wang, K.C. A guideline for 3D printing terminology in biomedical research utilizing ISO/ASTM standards. *3D Print. Med.* **2021**, *7*, 8. [CrossRef]
149. *ISO/ASTM52900-21*; Additive Manufacturing—General Principles—Fundamentals and Vocabulary. West ASTM International: Conshohocken, PA, USA, 2022; p. 14. [CrossRef]
150. Kam, D.; Chasnitsky, M.; Nowogrodski, C.; Braslavsky, I.; Abitbol, T.; Magdassi, S.; Shoseyov, O. Direct Cryo Writing of Aerogels via 3D Printing of Aligned Cellulose Nanocrystals Inspired by the Plant Cell Wall. *Colloid Interfac* **2019**, *3*, 46. [CrossRef]
151. Mendes, B.B.; Gómez-Florit, M.; Hamilton, A.G.; Detamore, M.S.; Domingues, R.M.A.; Reis, R.L.; Gomes, M.E. Human platelet lysate-based nanocomposite bioink for bioprinting hierarchical fibrillar structures. *Biofabrication* **2020**, *12*, 015012. [CrossRef] [PubMed]
152. Jiang, J.; Oguzlu, H.; Jiang, F. 3D printing of lightweight, super-strong yet flexible all-cellulose structure. *Chem. Eng. J.* **2021**, *405*, 126668. [CrossRef]
153. Guo, J.; Li, Q.; Zhang, R.; Li, B.; Zhang, J.; Yao, L.; Lin, Z.; Zhang, L.; Cao, X.; Duan, B. Loose Pre-Cross-Linking Mediating Cellulose Self-Assembly for 3D Printing Strong and Tough Biomimetic Scaffolds. *Biomacromolecules* **2022**, *23*, 877–888. [CrossRef] [PubMed]
154. Liu, G.; Bhat, M.P.; Kim, C.S.; Kim, J.; Lee, K.-H. Improved 3D-Printability of Cellulose Acetate to Mimic Water Absorption in Plant Roots through Nanoporous Networks. *Macromolecules* **2022**, *55*, 1855–1865. [CrossRef]
155. Esmaeili, M.; Norouzi, S.; George, K.; Rezvan, G.; Taheri-Qazvini, N.; Sadati, M. 3D Printing-Assisted Self-Assembly to Bio-Inspired Bouligand Nanostructures. *Small* **2023**, *2023*, 2206847. [CrossRef]
156. Raviv, D.; Zhao, W.; McKnelly, C.; Papadopoulou, A.; Kadambi, A.; Shi, B.; Hirsch, S.; Dikovsky, D.; Zyracki, M.; Olguin, C.; et al. Active Printed Materials for Complex Self-Evolving Deformations. *Sci. Rep.* **2014**, *4*, 7422. [CrossRef]
157. Tibbits, S. The emergence of "4D printing". In Proceedings of TED Conferences. Available online: https://youtu.be/0gMCZFHv9v8 (accessed on 20 December 2022).
158. Tibbits, S.; McKnelly, C.; Olguin, C.; Dikovsky, D.; Hirsch, S. 4D printing and universal transformation. In Proceedings of the 34th Annual Conference of the Association for Computer Aided Design in Architecture, Los Angeles, CA, USA, 23–25 October 2014; pp. 539–548.
159. Momeni, F.; Hassani.N, S.M.; Liu, X.; Ni, J. A review of 4D printing. *Mater. Des.* **2017**, *122*, 42–79. [CrossRef]
160. 4D Printing Market, by Application (Aerospace and Defense, Healthcare, Automotive, Construction, Clothing, Utility, Others.), by Region-Forecast to 2030. 2023, p. 100. Available online: https://www.precedenceresearch.com/4d-printing-market (accessed on 4 January 2023).
161. Gladman, A.S.; Matsumoto, E.A.; Nuzzo, R.G.; Mahadevan, L.; Lewis, J.A. Biomimetic 4D printing. *Nat. Mater.* **2016**, *15*, 413–418. [CrossRef]

162. Siqueira, G.; Kokkinis, D.; Libanori, R.; Hausmann, M.K.; Gladman, A.S.; Neels, A.; Tingaut, P.; Zimmermann, T.; Lewis, J.A.; Studart, A.R. Cellulose Nanocrystal Inks for 3D Printing of Textured Cellular Architectures. *Adv. Funct. Mater.* **2017**, *27*, 1604619. [CrossRef]
163. Zhao, X.; Tekinalp, H.; Meng, X.; Ker, D.; Benson, B.; Pu, Y.; Ragauskas, A.J.; Wang, Y.; Li, K.; Webb, E.; et al. Poplar as Biofiber Reinforcement in Composites for Large-Scale 3D Printing. *ACS Appl. Bio Mater.* **2019**, *2*, 4557–4570. [CrossRef]
164. Correa, D.; Papadopoulou, A.; Guberan, C.; Jhaveri, N.; Reichert, S.; Menges, A.; Tibbits, S. 3D-Printed Wood: Programming Hygroscopic Material Transformations. *3D Print Addit. Manuf.* **2015**, *2*, 106–116. [CrossRef]
165. Le Duigou, A.; Correa, D.; Ueda, M.; Matsuzaki, R.; Castro, M. A review of 3D and 4D printing of natural fibre biocomposites. *Mater. Des.* **2020**, *194*, 108911. [CrossRef]
166. Correa, D.; Poppinga, S.; Mylo, M.D.; Westermeier, A.S.; Bruchmann, B.; Menges, A.; Speck, T. 4D pine scale: Biomimetic 4D printed autonomous scale and flap structures capable of multi-phase movement. *Philos. Trans. A Math. Phys. Eng. Sci.* **2020**, *378*, 20190445. [CrossRef]
167. Mulakkal, M.C.; Trask, R.S.; Ting, V.P.; Seddon, A.M. Responsive cellulose-hydrogel composite ink for 4D printing. *Mater. Des.* **2018**, *160*, 108–118. [CrossRef]
168. Wang, W.; Yao, L.N.; Zhang, T.; Cheng, C.Y.; Levine, D.; Ishii, H. Transformative Appetite: Shape-Changing Food Transforms from 2D to 3D by Water Interaction through Cooking. In Proceedings of the 2017 ACM Sigchi Conference on Human Factors in Computing Systems (Chi'17), Denver, CO, USA, 6–11 May 2017; pp. 6123–6132. [CrossRef]
169. Teng, X.; Zhang, M.; Mujumdar, A.S. 4D printing: Recent advances and proposals in the food sector. *Trends Food Sci. Technol.* **2021**, *110*, 349–363. [CrossRef]
170. Navaf, M.; Sunooj, K.V.; Aaliya, B.; Akhila, P.P.; Sudheesh, C.; Mir, S.A.; George, J. 4D printing: A new approach for food printing; effect of various stimuli on 4D printed food properties. A comprehensive review. *Appl. Food Res.* **2022**, *2*, 100150. [CrossRef]
171. Lai, J.; Ye, X.; Liu, J.; Wang, C.; Li, J.; Wang, X.; Ma, M.; Wang, M. 4D printing of highly printable and shape morphing hydrogels composed of alginate and methylcellulose. *Mater. Des.* **2021**, *205*, 109699. [CrossRef]